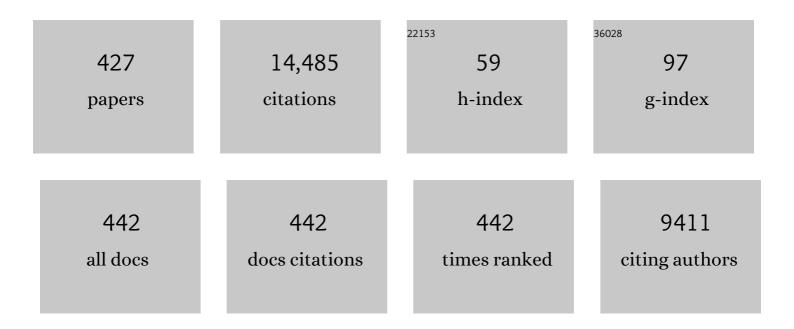
## Christina Trautmann

List of Publications by Year in descending order

Source: https://exaly.com/author-pdf/985218/publications.pdf Version: 2024-02-01



#	Article	IF	CITATIONS
1	Protein Biosensors Based on Biofunctionalized Conical Gold Nanotubes. Journal of the American Chemical Society, 2005, 127, 5000-5001.	13.7	491
2	Room-temperature entanglement between single defect spins in diamond. Nature Physics, 2013, 9, 139-143.	16.7	353
3	Fragmentation of nanowires driven by Rayleigh instability. Applied Physics Letters, 2004, 85, 5337-5339.	3.3	296
4	Swelling effects in lithium fluoride induced by swift heavy ions. Physical Review B, 2000, 62, 13-16.	3.2	267
5	Fine Structure in Swift Heavy Ion Tracks in Amorphous <mml:math xmlns:mml="http://www.w3.org/1998/Math/MathML" display="inline"&gt;<mml:msub><mml:mi>SiO</mml:mi><mml:mn>2</mml:mn></mml:msub>. Physical Review Letters, 2008, 101, 175503.</mml:math 	7.8	242
6	Track formation and fabrication of nanostructures with MeV-ion beams. Nuclear Instruments & Methods in Physics Research B, 2004, 216, 1-8.	1.4	235
7	An Asymmetric Polymer Nanopore for Single Molecule Detection. Nano Letters, 2004, 4, 497-501.	9.1	230
8	Review of A2B2O7 pyrochlore response to irradiation and pressure. Nuclear Instruments & Methods in Physics Research B, 2010, 268, 2951-2959.	1.4	202
9	Ultrafast ion sieving using nanoporous polymeric membranes. Nature Communications, 2018, 9, 569.	12.8	197
10	Preparation of synthetic nanopores with transport properties analogous to biological channels. Surface Science, 2003, 532-535, 1061-1066.	1.9	187
11	Highly Selective Ionic Transport through Subnanometer Pores in Polymer Films. Advanced Functional Materials, 2016, 26, 5796-5803.	14.9	182
12	Chemical modifications of PET induced by swift heavy ions. Nuclear Instruments & Methods in Physics Research B, 1997, 131, 159-166.	1.4	180
13	lon transport through asymmetric nanopores prepared by ion track etching. Nuclear Instruments & Methods in Physics Research B, 2003, 208, 143-148.	1.4	168
14	Electrical characterization of electrochemically grown single copper nanowires. Applied Physics Letters, 2003, 82, 2139-2141.	3.3	164
15	Single ion induced surface nanostructures: a comparison between slow highly charged and swift heavy ions. Journal of Physics Condensed Matter, 2011, 23, 393001.	1.8	157
16	Calcium-Induced Voltage Gating in Single Conical Nanopores. Nano Letters, 2006, 6, 1729-1734.	9.1	140
17	Nanometric transformation of the matter by short and intense electronic excitation: Experimental data versus inelastic thermal spike model. Nuclear Instruments & Methods in Physics Research B, 2012, 277, 28-39.	1.4	138
18	Jetlike Component in Sputtering of LiF Induced by Swift Heavy Ions. Physical Review Letters, 2002, 88, 057602	7.8	136

#	Article	IF	CITATIONS
19	Bioinspired integrated nanosystems based on solid-state nanopores: "iontronic―transduction of biological, chemical and physical stimuli. Chemical Science, 2017, 8, 890-913.	7.4	136
20	Electro-responsive asymmetric nanopores in polyimide with stable ion-current signal. Applied Physics A: Materials Science and Processing, 2003, 76, 781-785.	2.3	135
21	Polydopamine Meets Solid-State Nanopores: A Bioinspired Integrative Surface Chemistry Approach To Tailor the Functional Properties of Nanofluidic Diodes. Journal of the American Chemical Society, 2015, 137, 6011-6017.	13.7	131
22	Molecular Design of Solid‣tate Nanopores: Fundamental Concepts and Applications. Advanced Materials, 2019, 31, e1901483.	21.0	130
23	Single-ion tracks in <mml:math <br="" xmlns:mml="http://www.w3.org/1998/Math/MathML">display="inline"&gt;<mml:mrow><mml:msub><mml:mrow><mml:mtext>Gd</mml:mtext></mml:mrow><mml:mn>2 Physical Review B, 2009, 79, .</mml:mn></mml:msub></mml:mrow></mml:math>	< <b>þɔ₂</b> ml:mn	າ> <b>ະຊ<sub>ີ</sub>ອາກາໄ:</b> ກອ
24	Pore geometry of etched ion tracks in polyimide. Nuclear Instruments & Methods in Physics Research B, 1996, 111, 70-74.	1.4	114
25	Microstructured glass chip for ion-channel electrophysiology. Physical Review E, 2001, 64, 040901.	2.1	110
26	Structural modifications of Gd <sub>2</sub> Zr <sub>2-<i>x</i></sub> Ti <i><sub>x</sub></i> O <sub>7</sub> pyrochlore induced by swift heavy ions: Disordering and amorphization. Journal of Materials Research, 2009, 24, 1322-1334.	2.6	110
27	Damage and track morphology in LiF crystals irradiated with GeV ions. Physical Review B, 1998, 58, 11232-11240.	3.2	109
28	Damage structure in the ionic crystal LiF irradiated with swift heavy ions. Nuclear Instruments & Methods in Physics Research B, 2000, 164-165, 365-376.	1.4	103
29	Radiation damage in UO2 by swift heavy ions. Nuclear Instruments & Methods in Physics Research B, 1997, 122, 583-588.	1.4	101
30	Track size and track structure in polymer irradiated by heavy ions. Nuclear Instruments & Methods in Physics Research B, 1998, 146, 468-474.	1.4	101
31	3D tissue culture substrates produced by microthermoforming of pre-processed polymer films. Biomedical Microdevices, 2006, 8, 191-199.	2.8	100
32	Nanofluidic Diodes with Dynamic Rectification Properties Stemming from Reversible Electrochemical Conversions in Conducting Polymers. Journal of the American Chemical Society, 2015, 137, 15382-15385.	13.7	94
33	Highly Sensitive Biosensing with Solid-State Nanopores Displaying Enzymatically Reconfigurable Rectification Properties. Nano Letters, 2018, 18, 3303-3310.	9.1	91
34	Pyrolytic effects induced by energetic ions in polymers. Nuclear Instruments & Methods in Physics Research B, 1999, 151, 161-168.	1.4	90
35	Etched heavy ion tracks in polycarbonate as template for copper nanowires. Nuclear Instruments & Methods in Physics Research B, 2001, 185, 192-197.	1.4	90
36	Characterization of swift heavy ion tracks in CaF2 by scanning force and transmission electron microscopy. Nuclear Instruments & Methods in Physics Research B, 2005, 240, 819-828.	1.4	88

#	Article	IF	CITATIONS
37	Direct detection of human adenovirus or SARS-CoV-2 with ability to inform infectivity using DNA aptamer-nanopore sensors. Science Advances, 2021, 7, eabh2848.	10.3	87
38	Etching threshold for ion tracks in polyimide. Nuclear Instruments & Methods in Physics Research B, 1996, 116, 429-433.	1.4	85
39	Nanoscale manipulation of the properties of solids at high pressure with relativistic heavy ions. Nature Materials, 2009, 8, 793-797.	27.5	85
40	Host–guest supramolecular chemistry in solid-state nanopores: potassium-driven modulation of ionic transport in nanofluidic diodes. Nanoscale, 2015, 7, 15594-15598.	5.6	82
41	Color-center creation inLiFunder irradiation with swift heavy ions: Dependence on energy loss and fluence. Physical Review B, 2004, 70, .	3.2	80
42	Shape matters: Enhanced osmotic energy harvesting in bullet-shaped nanochannels. Nano Energy, 2020, 71, 104612.	16.0	80
43	Tracks of swift heavy ions in graphite studied by scanning tunneling microscopy. Physical Review B, 2001, 64, .	3.2	79
44	Polyimide microfluidic devices with integrated nanoporous filtration areas manufactured by micromachining and ion track technology. Journal of Micromechanics and Microengineering, 2004, 14, 324-331.	2.6	79
45	Chemical etching of ion tracks in LiF crystals. Journal of Applied Physics, 1998, 83, 3560-3564.	2.5	74
46	Electronic sputtering of metals and insulators by swift heavy ions. Nuclear Instruments & Methods in Physics Research B, 2003, 212, 346-357.	1.4	74
47	Redox response of actinide materials to highly ionizing radiation. Nature Communications, 2015, 6, 6133.	12.8	72
48	Effect of electronic energy loss and irradiation temperature on color-center creation in LiF and NaCl crystals irradiated with swift heavy ions. Physical Review B, 2008, 78, .	3.2	70
49	Flexible fluidic microchips based on thermoformed and locally modified thin polymer films. Lab on A Chip, 2008, 8, 1570.	6.0	69
50	An Allâ€Plastic Fieldâ€Effect Nanofluidic Diode Gated by a Conducting Polymer Layer. Advanced Materials, 2017, 29, 1700972.	21.0	68
51	Dense and nanometric electronic excitations induced by swift heavy ions in an ionic CaF2crystal: Evidence for two thresholds of damage creation. Physical Review B, 2012, 85, .	3.2	67
52	TiO <sub>2</sub> , SiO <sub>2</sub> , and Al <sub>2</sub> O <sub>3</sub> coated nanopores and nanotubes produced by ALD in etched ion-track membranes for transport measurements. Nanotechnology, 2015, 26, 335301.	2.6	67
53	Advances in understanding of swift heavy-ion tracks in complex ceramics. Current Opinion in Solid State and Materials Science, 2015, 19, 39-48.	11.5	66
54	Radiation defects in lithium fluoride induced by heavy ions. Nuclear Instruments & Methods in Physics Research B, 1998, 146, 367-378.	1.4	65

#	Article	IF	CITATIONS
55	Morphology of latent and etched heavy ion tracks in radiation resistant polymers polyimide and poly(ethylene naphthalate). Nuclear Instruments & Methods in Physics Research B, 2001, 185, 216-221.	1.4	65
56	Structural response of titanate pyrochlores to swift heavy ion irradiation. Acta Materialia, 2016, 117, 207-215.	7.9	64
57	Tracks of very heavy ions in polymers. Nuclear Instruments & Methods in Physics Research B, 1997, 131, 55-63.	1.4	62
58	Response of Gd2Ti2O7 and La2Ti2O7 to swift-heavy ion irradiation and annealing. Acta Materialia, 2015, 93, 1-11.	7.9	62
59	Colour centre production in yttria-stabilized zirconia by swift charged particle irradiations. Journal of Physics Condensed Matter, 2004, 16, 3957-3971.	1.8	60
60	Investigation of nanopore evolution in ion track-etched polycarbonate membranes. Nuclear Instruments & Methods in Physics Research B, 2007, 265, 553-557.	1.4	60
61	Similar local order in disordered fluorite and aperiodic pyrochlore structures. Acta Materialia, 2018, 144, 60-67.	7.9	60
62	Nanofluidic osmotic power generators – advanced nanoporous membranes and nanochannels for blue energy harvesting. Chemical Science, 2021, 12, 12874-12910.	7.4	60
63	Heavy-ion irradiation of pyrochlore oxides: Comparison between low and high energy regimes. Nuclear Instruments & Methods in Physics Research B, 2008, 266, 3043-3047.	1.4	59
64	Annealing kinetics of latent particle tracks in Durango apatite. Physical Review B, 2011, 83, .	3.2	59
65	Rectification properties of conically shaped nanopores: consequences of miniaturization. Physical Chemistry Chemical Physics, 2013, 15, 16917.	2.8	59
66	Nanoporous SiO2/Si thin layers produced by ion track etching: Dependence on the ion energy and criterion for etchability. Journal of Applied Physics, 2008, 104, .	2.5	58
67	Thermal annealing mechanisms of latent fission tracks: Apatite vs. zircon. Earth and Planetary Science Letters, 2011, 302, 227-235.	4.4	58
68	Electronic excitations and heavy-ion-induced processes in ionic crystals. Nuclear Instruments & Methods in Physics Research B, 2003, 209, 73-84.	1.4	57
69	Phosphateâ€Responsive Biomimetic Nanofluidic Diodes Regulated by Polyamine–Phosphate Interactions: Insights into Their Functional Behavior from Theory and Experiment. Small, 2018, 14, e1702131.	10.0	57
70	Preferred growth orientation of metallic fcc nanowires under direct and alternating electrodeposition conditions. Nanotechnology, 2007, 18, 135709.	2.6	55
71	Fabrication of nanoporous graphene/polymer composite membranes. Nanoscale, 2017, 9, 10487-10493.	5.6	55
72	Ion track diameters in mica studied with scanning force microscopy. Nuclear Instruments & Methods in Physics Research B, 1996, 107, 181-184.	1.4	53

#	Article	IF	CITATIONS
73	Role of composition, bond covalency, and short-range order in the disordering of stannate pyrochlores by swift heavy ion irradiation. Physical Review B, 2016, 94, .	3.2	53
74	Effect of Stress on Track Formation in Amorphous Iron Boron Alloy: Ion Tracks as Elastic Inclusions. Physical Review Letters, 2000, 85, 3648-3651.	7.8	52
75	Conductivity of nanometer-sized ion tracks in diamond-like carbon films. Journal of Applied Physics, 2003, 94, 1959-1964.	2.5	52
76	Creation of colour centres in diamond by collimated ionâ€implantation through nanoâ€channels in mica. Physica Status Solidi (A) Applications and Materials Science, 2011, 208, 2017-2022.	1.8	52
77	Phase Transitions in Solids Stimulated by Simultaneous Exposure to High Pressure and Relativistic Heavy Ions. Physical Review Letters, 2006, 96, 195701.	7.8	51
78	Thick optical waveguides in lithium niobate induced by swift heavy ions (~10 MeV/amu) at ultralow fluences. Optics Express, 2009, 17, 24175.	3.4	49
79	Optical spectroscopy study of damage induced in 4H-SiC by swift heavy ion irradiation. Journal of Physics Condensed Matter, 2012, 24, 125801.	1.8	49
80	Shrinking of Rapidly Evaporating Water Microdroplets Reveals their Extreme Supercooling. Physical Review Letters, 2018, 120, 015501.	7.8	49
81	Redox-Driven Reversible Gating of Solid-State Nanochannels. ACS Applied Materials & Interfaces, 2019, 11, 30001-30009.	8.0	49
82	Copper nanowires electrodeposited in etched single-ion track templates. Applied Physics A: Materials Science and Processing, 2003, 77, 751-755.	2.3	48
83	Creation of nanosize defects in LiF crystals under 5- and <mml:math xmlns:mml="http://www.w3.org/1998/Math/MathML" display="inline"&gt;<mml:mrow><mml:mn>10</mml:mn><mml:mtext>â^^</mml:mtext><mml:mi>MeV</mml:mi>ion irradiation at room temperature. Physical Review B. 2007, 76, .</mml:mrow></mml:math 	n <mark>312</mark> nml:mrow	>48mml:mat
84	Potential energy threshold for nano-hillock formation by impact of slow highly charged ions on a CaF2(111) surface. Nuclear Instruments & Methods in Physics Research B, 2007, 258, 167-171.	1.4	48
85	Swift heavy ion track formation in Gd2Zr2â~Ti O7 pyrochlore: Effect of electronic energy loss. Nuclear Instruments & Methods in Physics Research B, 2014, 336, 102-115.	1.4	48
86	Degradation of polyimide under irradiation with swift heavy ions. Nuclear Instruments & Methods in Physics Research B, 2005, 236, 456-460.	1.4	47
87	Structural phase transition in induced by swift heavy ion irradiation at high-pressure. Nuclear Instruments & Methods in Physics Research B, 2009, 267, 964-968.	1.4	47
88	Evidence of blocking effects on 3-keV Ne <mml:math xmlns:mml="http://www.w3.org/1998/Math/MathML" display="inline"&gt;<mml:mrow><mml:msup><mml:mrow /&gt;<mml:mrow><mml:mn>7+</mml:mn></mml:mrow></mml:mrow </mml:msup></mml:mrow><td>2.5 ath&gt;ions</td><td>47</td></mml:math 	2.5 ath>ions	47
89	Noncovalent functionalization of solid-state nanopores via self-assembly of amphipols. Nanoscale, 2016, 8, 1470-1478.	5.6	47
90	Biomimetic solid-state nanochannels for chemical and biological sensing applications. TrAC - Trends in Analytical Chemistry, 2021, 144, 116425.	11.4	47

6

#	Article	IF	CITATIONS
91	Applied nuclear physics at the new high-energy particle accelerator facilities. Physics Reports, 2019, 800, 1-37.	25.6	46
92	Specificity of ion induced damage. Nuclear Instruments & Methods in Physics Research B, 1999, 156, 162-169.	1.4	45
93	Grain size effects on irradiated CeO2, ThO2, and UO2. Acta Materialia, 2018, 160, 47-56.	7.9	45
94	Ion-induced formation of colloids in LiF at 15 K. Physical Review B, 1997, 56, 10711-10714.	3.2	44
95	Swelling of insulators induced by swift heavy ions. Nuclear Instruments & Methods in Physics Research B, 2002, 191, 144-148.	1.4	44
96	Study of the damage produced in CaF2 by swift heavy ion irradiation. Nuclear Instruments & Methods in Physics Research B, 2002, 191, 301-305.	1.4	44
97	On the nano-hillock formation induced by slow highly charged ions on insulator surfaces. Solid-State Electronics, 2007, 51, 1398-1404.	1.4	44
98	Irradiation-induced stabilization of zircon (ZrSiO4) at high pressure. Earth and Planetary Science Letters, 2008, 269, 291-295.	4.4	44
99	Forging Fast Ion Conducting Nanochannels with Swift Heavy Ions: The Correlated Role of Local Electronic and Atomic Structure. Journal of Physical Chemistry C, 2017, 121, 975-981.	3.1	44
100	Guided transmission ofNe7+ions through nanocapillaries in insulating polymers: Scaling laws for projectile energies up to 50 keV. Physical Review A, 2009, 79, .	2.5	42
101	Amorphization of nanocrystalline monoclinic ZrO2 by swift heavy ion irradiation. Physical Chemistry Chemical Physics, 2012, 14, 12295.	2.8	42
102	SAXS investigations of the morphology of swift heavy ion tracks in α-quartz. Journal of Physics Condensed Matter, 2013, 25, 045006.	1.8	41
103	Defect accumulation in ThO2 irradiated with swift heavy ions. Nuclear Instruments & Methods in Physics Research B, 2014, 326, 169-173.	1.4	41
104	APPA at FAIR: From fundamental to applied research. Nuclear Instruments & Methods in Physics Research B, 2015, 365, 680-685.	1.4	41
105	Phase transformations in <mml:math xmlns:mml="http://www.w3.org/1998/Math/MathML"&gt;<mml:mrow><mml:msub><mml:mi>Ln</mml:mi><mml: mathvariant="normal"&gt;O<mml:mn>3</mml:mn></mml: </mml:msub></mml:mrow>materials irradiated with swift heavy ions. Physical Review B. 2015. 92</mml:math 	nn>23.2	nl:mn>
106	MeV gold irradiation induced damage in α-quartz: Competition between nuclear and electronic stopping. Nuclear Instruments & Methods in Physics Research B, 2001, 178, 331-336.	1.4	40
107	Confined fission tracks in ion-irradiated and step-etched prismatic sections of Durango apatite. Chemical Geology, 2007, 242, 202-217.	3.3	40
108	Fission tracks simulated by swift heavy ions at crustal pressures and temperatures. Earth and Planetary Science Letters, 2008, 274, 355-358.	4.4	40

#	Article	IF	CITATIONS
109	Study of heavy-ion induced modifications in BaF2 and LaF3 single crystals. Nuclear Instruments & Methods in Physics Research B, 2004, 218, 492-497.	1.4	39
110	Cylindrical nanochannels in ion-track polycarbonate membranes studied by small-angle X-ray scattering. Journal of Applied Crystallography, 2007, 40, s388-s392.	4.5	39
111	Multipole Surface Plasmon Resonances in Conductively Coupled Metal Nanowire Dimers. ACS Nano, 2012, 6, 9711-9717.	14.6	39
112	Amine-Phosphate Specific Interactions within Nanochannels: Binding Behavior and Nanoconfinement Effects. Journal of Physical Chemistry C, 2019, 123, 28997-29007.	3.1	39
113	Polyaniline for Improved Blue Energy Harvesting: Highly Rectifying Nanofluidic Diodes Operating in Hypersaline Conditions via One-Step Functionalization. ACS Applied Materials & Interfaces, 2020, 12, 28148-28157.	8.0	39
114	Effect of ion irradiation and heat treatment on adhesion in the Cu / Teflon system. Journal of Adhesion Science and Technology, 1995, 9, 1523-1529.	2.6	38
115	Track structure in polyethylene terephthalate irradiated by heavy ions: Let dependence of track diameter. Radiation Measurements, 1999, 31, 51-56.	1.4	38
116	Field emission properties of electrochemically deposited gold nanowires. Applied Physics Letters, 2008, 92, 063115.	3.3	38
117	Nanopores in track-etched polymer membranes characterized by small-angle x-ray scattering. Nanotechnology, 2010, 21, 155702.	2.6	38
118	Observation and chemical treatment of heavy-ion tracks in polymers. Nuclear Instruments & Methods in Physics Research B, 1995, 105, 81-85.	1.4	37
119	Electronic Sputtering with Swift Heavy Ions. , 2007, , 401-450.		37
120	Response behavior of ZrO2 under swift heavy ion irradiation with and without external pressure. Nuclear Instruments & Methods in Physics Research B, 2012, 277, 45-52.	1.4	37
121	The Influence of Divalent Anions on the Rectification Properties of Nanofluidic Diodes: Insights from Experiments and Theoretical Simulations. ChemPhysChem, 2016, 17, 2718-2725.	2.1	37
122	Vertically-Aligned Single-Crystal Nanocone Arrays: Controlled Fabrication and Enhanced Field Emission. ACS Applied Materials & Interfaces, 2016, 8, 472-479.	8.0	37
123	Noncovalent Approach toward the Construction of Nanofluidic Diodes with pH-Reversible Rectifying Properties: Insights from Theory and Experiment. Journal of Physical Chemistry C, 2017, 121, 9070-9076.	3.1	37
124	Chemical degradation of polyimide and polysulfone films under the irradiation with heavy ions of several hundred meV. Journal of Polymer Science Part A, 1999, 37, 4318-4329.	2.3	36
125	Field emission of copper nanowires grown in polymer ion-track membranes. Nuclear Instruments & Methods in Physics Research B, 2006, 245, 337-341.	1.4	36
126	Characterization of ion-induced radiation effects in nuclear materials using synchrotron x-ray techniques. Journal of Materials Research, 2015, 30, 1366-1379.	2.6	36

#	Article	IF	CITATIONS
127	Defect accumulation in swift heavy ion-irradiated CeO <sub>2</sub> and ThO <sub>2</sub> . Journal of Materials Chemistry A, 2017, 5, 12193-12201.	10.3	36
128	Discontinuous tracks in arsenic-doped crystallineSi0.5Ge0.5alloy layers. Physical Review B, 2002, 66, .	3.2	35
129	Swift heavy ion-induced swelling and damage in yttria-stabilized zirconia. Journal of Applied Physics, 2007, 101, 073501.	2.5	35
130	Scanning force microscopy of heavy-ion tracks in lithium fluoride. Nuclear Instruments & Methods in Physics Research B, 1998, 146, 393-398.	1.4	34
131	Protonâ€Gated Rectification Regimes in Nanofluidic Diodes Switched by Chemical Effectors. Small, 2018, 14, e1703144.	10.0	34
132	Heavy Ion Radiation Effects on Hafnium Oxide-Based Resistive Random Access Memory. IEEE Transactions on Nuclear Science, 2019, 66, 1715-1718.	2.0	34
133	Shape of nanopores in track-etched polycarbonate membranes. Journal of Membrane Science, 2021, 638, 119681.	8.2	34
134	Microthermoforming as a novel technique for manufacturing scaffolds in tissue engineering (CellChips®). IET Nanobiotechnology, 2004, 151, 151.	2.1	33
135	Swift heavy ion-induced amorphization of CaZrO3 perovskite. Nuclear Instruments & Methods in Physics Research B, 2012, 286, 271-276.	1.4	33
136	Investigation of heavy ion tracks in polymers by transmission electron microscopy. Nuclear Instruments & Methods in Physics Research B, 2001, 185, 210-215.	1.4	32
137	Color center creation in LiF crystals irradiated with 5- and 10-MeV Au ions. Nuclear Instruments & Methods in Physics Research B, 2008, 266, 2736-2740.	1.4	32
138	Tailoring of keV-Ion Beams by Image Charge when Transmitting through Rhombic and Rectangular Shaped Nanocapillaries. Physical Review Letters, 2012, 108, 193202.	7.8	32
139	Silver nanostructures formation in porous Si/SiO2 matrix. Journal of Crystal Growth, 2014, 400, 21-26.	1.5	32
140	Conformal SiO2 coating of sub-100 nm diameter channels of polycarbonate etched ion-track channels by atomic layer deposition. Beilstein Journal of Nanotechnology, 2015, 6, 472-479.	2.8	32
141	Characterization of heavy ion tracks in polymers by transmission electron microscopy. Journal of Polymer Science, Part B: Polymer Physics, 2003, 41, 2892-2901.	2.1	31
142	Discontinuous tracks in relaxed Si0.5Ge0.5 alloy layers: A velocity effect. Applied Physics Letters, 2003, 83, 1746-1748.	3.3	31
143	Raman spectroscopy of apatite irradiated with swift heavy ions with and without simultaneous exertion of high pressure. Applied Physics A: Materials Science and Processing, 2008, 91, 17-22.	2.3	31
144	Swift heavy ion-induced phase transformation in Gd2O3. Nuclear Instruments & Methods in Physics Research B, 2014, 326, 121-125.	1.4	31

#	Article	IF	CITATIONS
145	Liquid-like phase formation in Gd2Zr2O7 by extremely ionizing irradiation. Journal of Applied Physics, 2009, 105, .	2.5	30
146	Morphology of swift heavy ion tracks in metallic glasses. Journal of Non-Crystalline Solids, 2012, 358, 571-576.	3.1	30
147	Confinement Effects of Ion Tracks in Ultrathin Polymer Films. Physical Review Letters, 2015, 114, 118302.	7.8	30
148	Surface Enrichment in Au–Ag Alloy Nanowires and Investigation of the Dealloying Process. Journal of Physical Chemistry C, 2015, 119, 20949-20956.	3.1	30
149	Electrodeposition and electroless plating of hierarchical metal superstructures composed of 1D nano- and microscale building blocks. Electrochimica Acta, 2016, 202, 47-54.	5.2	30
150	Towards a nanostructured thermoelectric generator using ion-track lithography. Journal of Micromechanics and Microengineering, 2008, 18, 104015.	2.6	29
151	Characterization of swift heavy ion irradiation damage in ceria. Journal of Materials Research, 2015, 30, 1473-1484.	2.6	29
152	Shedding light on the mechanism of asymmetric track etching: an interplay between latent track structure, etchant diffusion and osmotic flow. Physical Chemistry Chemical Physics, 2016, 18, 25421-25433.	2.8	29
153	Vacuum ultraviolet absorption and ion track effects in LiF crystals irradiated with swift ions. Physical Review B, 2002, 66, .	3.2	28
154	STM and Raman spectroscopic study of graphite irradiated by heavy ions. Nuclear Instruments & Methods in Physics Research B, 2003, 212, 303-307.	1.4	28
155	CHARGE SPECTRUM OF HEAVY AND SUPERHEAVY COMPONENTS OF GALACTIC COSMIC RAYS: RESULTS OF THE OLIMPIYA EXPERIMENT. Astrophysical Journal, 2016, 829, 120.	4.5	28
156	Stopping power dependence of ion track etching in amorphous metallic Fe81B13.5 Si3.5C2. Nuclear Instruments & Methods in Physics Research B, 1993, 83, 513-517.	1.4	27
157	Etching of nanopores in polycarbonate irradiated with swift heavy ions at 15K. Nuclear Instruments & Methods in Physics Research B, 2006, 245, 284-287.	1.4	27
158	Surface nanostructuring of SrTiO3 single crystals by slow highly charged ions and swift heavy ions. Nuclear Instruments & Methods in Physics Research B, 2011, 269, 1234-1237.	1.4	27
159	Radiolysis and sputtering of carbon dioxide ice induced by swift Ti, Ni, and Xe ions. Nuclear Instruments & Methods in Physics Research B, 2015, 365, 477-481.	1.4	27
160	Study of ion beam induced swelling in fluorite as an inert matrix model. Progress in Nuclear Energy, 2001, 38, 271-274.	2.9	26
161	Heavy-ion induced damage in fluorite nanopowder. Nuclear Instruments & Methods in Physics Research B, 2001, 175-177, 590-593.	1.4	26
162	Magnetic and optical properties of cobalt nanowires fabricated in polycarbonate ion-track templates. Nuclear Instruments & Methods in Physics Research B, 2009, 267, 2567-2570.	1.4	26

#	Article	IF	CITATIONS
163	Nano-hillock formation in diamond-like carbon induced by swift heavy projectiles in the electronic stopping regime: Experiments and atomistic simulations. Applied Physics Letters, 2012, 101, .	3.3	26
164	Effect of spatial redistribution of valence holes on the formation of a defect halo of swift heavy-ion tracks in LiF. Physical Review B, 2013, 87, .	3.2	26
165	Effect of orientation on ion track formation in apatite and zircon. American Mineralogist, 2014, 99, 1127-1132.	1.9	26
166	Nanoscale density variations induced by high energy heavy ions in amorphous silicon nitride and silicon dioxide. Nanotechnology, 2018, 29, 144004.	2.6	26
167	Damage produced in magnesium aluminate spinel by high energy heavy ions including fission products of fission energy: microstructure modifications. Progress in Nuclear Energy, 2001, 38, 281-286.	2.9	25
168	Hardening and long-range stress formation in lithium fluoride induced by energetic ions. Nuclear Instruments & Methods in Physics Research B, 2003, 209, 93-97.	1.4	25
169	The effect of columnar defects on the pinning properties of NdFeAsO <sub>0.85</sub> conglomerate particles. Superconductor Science and Technology, 2009, 22, 125023.	3.5	25
170	Effect of irradiation parameters on defect aggregation during thermal annealing of LiF irradiated with swift ions and electrons. Physical Review B, 2010, 82, .	3.2	25
171	Swift heavy ion irradiation-induced amorphization of La2Ti2O7. Nuclear Instruments & Methods in Physics Research B, 2014, 326, 145-149.	1.4	25
172	<i>In situ</i> defect annealing of swift heavy ion irradiated CeO <sub>2</sub> and ThO <sub>2</sub> using synchrotron X-ray diffraction and a hydrothermal diamond anvil cell. Journal of Applied Crystallography, 2015, 48, 711-717.	4.5	25
173	Out-of-plane swelling of gadolinium gallium garnet induced by swift heavy ions. Nuclear Instruments & Methods in Physics Research B, 1998, 146, 426-430.	1.4	24
174	Micro- and Nanoengineering with Ion Tracks. Particle Acceleration and Detection, 2009, , 369-387.	0.5	24
175	On the morphology of Si/SiO2/Ni nanostructures with swift heavy ion tracks in silicon oxide. Journal of Surface Investigation, 2014, 8, 805-813.	0.5	23
176	Fundamental Phenomena and Applications of Swift Heavy Ion Irradiations. , 2020, , 485-516.		23
177	Porous fission fragment tracks in fluorapatite. Physical Review B, 2010, 82, .	3.2	22
178	Size characterization of ion tracks in PET and PTFE using SAXS. Nuclear Instruments & Methods in Physics Research B, 2015, 365, 573-577.	1.4	22
179	Porous Gold Nanowires: Plasmonic Response and Surfaceâ€Enhanced Infrared Absorption. Advanced Optical Materials, 2016, 4, 1838-1845.	7.3	22
180	Amorphization of Ta2O5 under swift heavy ion irradiation. Nuclear Instruments & Methods in Physics Research B, 2017, 407, 25-33.	1.4	22

#	Article	IF	CITATIONS
181	ZnO Nanowire Networks as Photoanode Model Systems for Photoelectrochemical Applications. Nanomaterials, 2018, 8, 693.	4.1	22
182	Zinc ion driven ionic conduction through single asymmetric nanochannels functionalized with nanocomposites. Electrochimica Acta, 2020, 337, 135810.	5.2	22
183	Electrochemically addressable nanofluidic devices based on PET nanochannels modified with electropolymerized poly- <i>o</i> -aminophenol films. Nanoscale, 2020, 12, 6002-6011.	5.6	22
184	Scanning tunneling microscopy of surface modifications induced by UNILAC heavy-ion irradiation. Ultramicroscopy, 1992, 42-44, 1345-1349.	1.9	21
185	GeV heavy ion induced adhesion enhancement. Nuclear Instruments & Methods in Physics Research B, 1993, 83, 503-507.	1.4	21
186	Influence of the spatial and temporal structure of the deposited-energy distribution in swift-ion-induced sputtering. Physical Review B, 2003, 68, .	3.2	21
187	X-ray diffraction study of the damage induced in yttria-stabilized zirconia by swift heavy ion irradiations. Journal of Applied Physics, 2008, 104, .	2.5	21
188	Copper nanocones grown in polymer ion-track membranes as field emitters. EPJ Applied Physics, 2012, 58, 10402.	0.7	21
189	SAXS and TEM investigation of ion tracks in neodymium-doped yttrium aluminium garnet. Nuclear Instruments & Methods in Physics Research B, 2014, 326, 150-153.	1.4	21
190	Observation of etched tracks in an amorphous metal. Radiation Effects and Defects in Solids, 1993, 126, 207-210.	1.2	20
191	Influence of temperature during irradiation on the structure of latent track in polycarbonate. Radiation Measurements, 2009, 44, 759-762.	1.4	20
192	Formation of surface nanostructures on rutile (TiO <sub>2</sub> ): comparative study of low-energy cluster ion and high-energy monoatomic ion impact. Journal Physics D: Applied Physics, 2009, 42, 205303.	2.8	20
193	The shape of ion tracks in natural apatite. Nuclear Instruments & Methods in Physics Research B, 2014, 326, 117-120.	1.4	20
194	Electronic sputtering of vitreous SiO2: Experimental and modeling results. Nuclear Instruments & Methods in Physics Research B, 2016, 379, 2-8.	1.4	20
195	Synergistically-enhanced ion track formation in pre-damaged strontium titanate by energetic heavy ions. Acta Materialia, 2018, 150, 351-359.	7.9	20
196	High-sensitivity detection of dopamine by biomimetic nanofluidic diodes derivatized with poly(3-aminobenzylamine). Nanoscale, 2020, 12, 18390-18399.	5.6	20
197	Effect of radial energy distribution on ion track etching in amorphous metallic Fe81B13.5Si3.5C2. Nuclear Instruments & Methods in Physics Research B, 1996, 108, 94-98.	1.4	19
198	Conductivity of ion tracks in diamond-like carbon films. Diamond and Related Materials, 2003, 12, 938-941.	3.9	19

#	Article	IF	CITATIONS
199	Swelling and creation of color centers in MgF2 single crystals irradiated with energetic heavy ions. Nuclear Instruments & Methods in Physics Research B, 2006, 245, 250-254.	1.4	19
200	Efficient field emission from structured gold nanowire cathodes. EPJ Applied Physics, 2009, 48, 30502.	0.7	19
201	Outgassing and degradation of polyimide induced by swift heavy ion irradiation at cryogenic temperature. Journal of Applied Physics, 2010, 108, .	2.5	19
202	Phase field modelling of dynamic thermal fracture in the context of irradiation damage. Continuum Mechanics and Thermodynamics, 2017, 29, 977-988.	2.2	19
203	Charge-state related effects in sputtering of LiF by swift heavy ions. Nuclear Instruments & Methods in Physics Research B, 2017, 392, 94-101.	1.4	19
204	Osmotic Effects in Trackâ€Etched Nanopores. Small, 2018, 14, e1703327.	10.0	19
205	Hardening and formation of dislocation structures in LiF crystals irradiated with MeV–GeV ions. Nuclear Instruments & Methods in Physics Research B, 2002, 196, 299-307.	1.4	18
206	Structural modifications induced by swift heavy ions in cubic stabilized zirconia: An X-ray diffraction investigation. Nuclear Instruments & Methods in Physics Research B, 2007, 257, 476-479.	1.4	18
207	Displacive radiation-induced structural contraction in nanocrystalline ZrN. Applied Physics Letters, 2012, 101, 041904.	3.3	18
208	Temperature dependence of ion track formation in quartz and apatite. Journal of Applied Crystallography, 2013, 46, 1558-1563.	4.5	18
209	Self‣upporting Metal Nanotube Networks Obtained by Highly Conformal Electroless Plating. ChemPlusChem, 2015, 80, 1448-1456.	2.8	18
210	The Effect of Heavy Ion Irradiation on the Forward Dissolution Rate of Borosilicate Glasses Studied In Situ and Real Time by Fluid-Cell Raman Spectroscopy. Materials, 2019, 12, 1480.	2.9	18
211	Scanning force microscopy of heavy-ion induced damage in lanthanum fluoride single crystals. Surface and Coatings Technology, 2002, 158-159, 522-525.	4.8	17
212	Energy loss of 50-GeV uranium ions in natural diamond. Applied Physics A: Materials Science and Processing, 2005, 80, 691-694.	2.3	17
213	Enhancement of etch rate for preparation of nano-sized ion-track membranes of poly(vinylidene) Tj ETQq1 1 0.78 Physics Research B, 2009, 267, 554-557.	4314 rgBT 1.4	Överlock 1 17
214	Investigation of initial stage of chemical etching of ion tracks in polycarbonate. Nuclear Instruments & Methods in Physics Research B, 2009, 267, 1039-1044.	1.4	17
215	Tuning the conductivity of vanadium dioxide films on silicon by swift heavy ion irradiation. AIP Advances, 2011, 1, .	1.3	17
216	Effect of doping on the radiation response of conductive Nb–SrTiO3. Nuclear Instruments & Methods in Physics Research B, 2013, 302, 40-47.	1.4	17

#	Article	IF	CITATIONS
217	Influence of electrodeposition parameters on the structure and morphology of ZnO nanowire arrays and networks synthesized in etched ion-track membranes. Semiconductor Science and Technology, 2016, 31, 014006.	2.0	17
218	Influence of surface states and size effects on the Seebeck coefficient and electrical resistance of Bi1â°'xSbxnanowire arrays. Nanoscale, 2017, 9, 3169-3179.	5.6	17
219	Swift heavy ion irradiation of interstellar dust analogues. Astronomy and Astrophysics, 2017, 599, A130.	5.1	17
220	Swelling of SiO <sub>2</sub> Quartz Induced by Energetic Heavy Ions. Materials Research Society Symposia Proceedings, 1997, 504, 123.	0.1	16
221	Heavy-ion induced modification of lithium fluoride observed by scanning force microscopy. Applied Physics A: Materials Science and Processing, 1998, 66, S1147-S1150.	2.3	16
222	Field emission enhancement by graphitic nano-scale channels through ta-C layers. Diamond and Related Materials, 2003, 12, 469-473.	3.9	16
223	Thermal spike effect on defect evolution in NaCl irradiated with light and heavy ions at 8 and 300K. Nuclear Instruments & Methods in Physics Research B, 2006, 245, 204-209.	1.4	16
224	Raman study of apatite amorphised with swift heavy ions under various irradiation conditions. Physics and Chemistry of Minerals, 2011, 38, 293-303.	0.8	16
225	Release of large polycyclic aromatic hydrocarbons and fullerenes by cosmic rays from interstellar dust. Astronomy and Astrophysics, 2019, 623, A134.	5.1	16
226	Modeling of primary defect aggregation in tracks of swift heavy ions in LiF. Physical Review B, 2001, 64,	3.2	15
227	Heavy-ion irradiation on crystallographically oriented cordierite and the conversion of molecular CO2 to CO: a Raman spectroscopic study. Physics and Chemistry of Minerals, 2010, 37, 417-424.	0.8	15
228	Electronic sputtering of Gd3Ga5O12 and Y3Fe5O12 garnets: Yield, stoichiometry and comparison to track formation. Nuclear Instruments & Methods in Physics Research B, 2011, 269, 955-958.	1.4	15
229	SAXS study of ion tracks in San Carlos olivine and Durango apatite. Nuclear Instruments & Methods in Physics Research B, 2012, 286, 243-246.	1.4	15
230	Areal density effects on the blocking of 3-keV Ne7+ions guided through nanocapillaries in polymers. Physical Review A, 2013, 88, .	2.5	15
231	Local formation of nitrogen-vacancy centers in diamond by swift heavy ions. Journal of Applied Physics, 2014, 116, .	2.5	15
232	Irradiation effects in CaF <sub>2</sub> probed by Raman scattering. Journal of Raman Spectroscopy, 2016, 47, 978-983.	2.5	15
233	Fabrication and thermoelectrical characterization of threeâ€dimensional nanowire networks. Physica Status Solidi (A) Applications and Materials Science, 2016, 213, 610-619.	1.8	15
234	Data consistencies of swift heavy ion induced damage creation in yttrium iron garnet analyzed by different techniques. Nuclear Instruments & Methods in Physics Research B, 2016, 366, 155-160.	1.4	15

#	Article	IF	CITATIONS
235	Anisotropic expansion and amorphization of Ga2O3 irradiated with 946 MeV Au ions. Nuclear Instruments & Methods in Physics Research B, 2016, 374, 40-44.	1.4	15
236	SAXS investigation of un-etched and etched ion tracks in polycarbonate. Nuclear Instruments & Methods in Physics Research B, 2017, 409, 293-297.	1.4	15
237	lonoacoustic detection of swift heavy ions. Nuclear Instruments and Methods in Physics Research, Section A: Accelerators, Spectrometers, Detectors and Associated Equipment, 2020, 950, 162935.	1.6	15
238	Solvent induced track sensitization. Extraction of oligomers. Nuclear Instruments & Methods in Physics Research B, 1994, 86, 325-332.	1.4	14
239	Heavy ion induced damage in NaCl and KCl crystals. Nuclear Instruments & Methods in Physics Research B, 2005, 229, 397-405.	1.4	14
240	Ion tracks in apatite at high pressures: the effect of crystallographic track orientation on the elastic properties of fluorapatite under hydrostatic compression. Physics and Chemistry of Minerals, 2010, 37, 371-387.	0.8	14
241	Generation of colour centres in yttria-stabilized zirconia by heavy ion irradiations in the GeV range. Journal of Physics Condensed Matter, 2010, 22, 315402.	1.8	14
242	Surface nanostructuring of LiNbO3 by high-density electronic excitations. Nuclear Instruments & Methods in Physics Research B, 2013, 315, 265-268.	1.4	14
243	Modeling of defect accumulation in lithium fluoride crystals under irradiation with swift ions. Nuclear Instruments & Methods in Physics Research B, 2014, 326, 307-310.	1.4	14
244	Insights on dramatic radial fluctuations in track formation by energetic ions. Scientific Reports, 2016, 6, 27196.	3.3	14
245	Degradation of thermal transport properties in fine-grained isotropic graphite exposed to swift heavy ion beams. Acta Materialia, 2020, 184, 187-198.	7.9	14
246	Efficient Chiral Nanosenor Based on Tip-Modified Nanochannels. Analytical Chemistry, 2021, 93, 6145-6150.	6.5	14
247	Polymerization of pyrrole into track membranes. Nuclear Instruments & Methods in Physics Research B, 1995, 105, 204-207.	1.4	13
248	Modifications induced by swift heavy ions. Bulletin of Materials Science, 1999, 22, 679-686.	1.7	13
249	Investigating carbon materials for use as the electron emission source in a parallel electron-beam lithography system. Current Applied Physics, 2001, 1, 317-320.	2.4	13
250	Effect of alloy composition on track formation in relaxed Si1â^'xGex. Physica B: Condensed Matter, 2003, 340-342, 808-812.	2.7	13
251	Pipetting Nanowires: In Situ Visualization of Solidâ€State Nanowireâ€ŧoâ€Nanoparticle Transformation Driven by Surface Diffusionâ€Mediated Capillarity. Advanced Functional Materials, 2012, 22, 695-701.	14.9	13
252	Polycarbonate activation for electroless plating by dimethylaminoborane absorption and subsequent nanoparticle deposition. Applied Physics A: Materials Science and Processing, 2014, 116, 287-294.	2.3	13

#	Article	IF	CITATIONS
253	STEM-EELS analysis of multipole surface plasmon modes in symmetry-broken AuAg nanowire dimers. Nanoscale, 2015, 7, 4935-4941.	5.6	13
254	Exploring the Electronic Structure and Chemical Homogeneity of Individual Bi <sub>2</sub> Te <sub>3</sub> Nanowires by Nano-Angle-Resolved Photoemission Spectroscopy. Nano Letters, 2016, 16, 4001-4007.	9.1	13
255	New insights on ion track morphology in pyrochlores by aberration corrected scanning transmission electron microscopy. Journal of Materials Research, 2017, 32, 928-935.	2.6	13
256	Structure, morphology and annealing behavior of ion tracks in polycarbonate. European Polymer Journal, 2018, 108, 406-411.	5.4	13
257	Etched ion tracks in amorphous SiO <sub>2</sub> characterized by small angle x-ray scattering: influence of ion energy and etching conditions. Nanotechnology, 2019, 30, 274001.	2.6	13
258	Track etching in amorphous metallic Fe81B13.5Si3.5C2. Nuclear Instruments & Methods in Physics Research B, 1996, 107, 397-402.	1.4	12
259	Graphite irradiated by swift heavy ions under grazing incidence. Nuclear Instruments & Methods in Physics Research B, 2002, 193, 259-264.	1.4	12
260	Heavy ion induced damage in MgF 2 crystals. Radiation Effects and Defects in Solids, 2002, 157, 649-654.	1.2	12
261	Conductive nanoscopic ion-tracks in diamond-like-carbon. Materials Science and Engineering C, 2006, 26, 1171-1174.	7.3	12
262	Storage efficiency of BaFBr:Eu2+ image plates irradiated by swift heavy ions. Journal of Luminescence, 2007, 125, 40-44.	3.1	12
263	Raman spectroscopy of heavy ion induced damage in cordierite. Nuclear Instruments & Methods in Physics Research B, 2008, 266, 2990-2993.	1.4	12
264	Self-aligned nanostructures created by swift heavy ion irradiation. Journal of Applied Physics, 2010, 107, 094305.	2.5	12
265	Photobleaching setup for the biological end-station of the darmstadt heavy-ion microprobe. Nuclear Instruments & Methods in Physics Research B, 2013, 306, 81-84.	1.4	12
266	Tailored nanochannels of nearly cylindrical geometry analysed by small angle X-ray scattering. Applied Physics A: Materials Science and Processing, 2014, 114, 387-392.	2.3	12
267	Surface plasmonic spectroscopy revealing the oxidation dynamics of copper nanowires embedded in polycarbonate ion-track templates. Journal of Materials Chemistry C, 2016, 4, 3956-3962.	5.5	12
268	Effects of Size Reduction on the Electrical Transport Properties of 3D Bi Nanowire Networks. Advanced Electronic Materials, 2021, 7, 2001069.	5.1	12
269	Defect-Induced Phase Transition in Hafnium Oxide Thin Films: Comparing Heavy Ion Irradiation and Oxygen-Engineering Effects. IEEE Transactions on Nuclear Science, 2021, 68, 1542-1547.	2.0	12
270	Biopolymerâ€Templated Deposition of Ordered and Polymorph Titanium Dioxide Thin Films for Improved Surfaceâ€Enhanced Raman Scattering Sensitivity. Advanced Functional Materials, 2022, 32, 2108556.	14.9	12

#	Article	IF	CITATIONS
271	Scanning force microscopy of heavy-ion tracks. Radiation Effects and Defects in Solids, 1993, 126, 213-216.	1.2	11
272	Solvent-induced sensitization of ion tracks in PET analyzed by small-angle X-ray scattering and differential scanning calorimetry. Nuclear Instruments & Methods in Physics Research B, 1995, 105, 200-203.	1.4	11
273	Ion tracks in mica studied with scanning force microscopy using force modulation. Nuclear Instruments & Methods in Physics Research B, 1996, 116, 492-495.	1.4	11
274	Paramagnetic centers induced in cubic zirconia by 2.5-MeV electron and 2.6-GeV uranium ion irradiations. Nuclear Instruments & Methods in Physics Research B, 2002, 191, 616-621.	1.4	11
275	SFM study of ion-induced hillocks on LiF exposed to thermal and optical annealing. Nuclear Instruments & Methods in Physics Research B, 2003, 209, 175-178.	1.4	11
276	Transmission of highly charged ions through mica nanocapillaries of rhombic cross section. Physical Review A, 2012, 86, .	2.5	11
277	Influence of swift heavy ion beams and protons on the dielectric strength ofÂpolyimide. Polymer Degradation and Stability, 2012, 97, 2396-2402.	5.8	11
278	Hierarchically porous carbon membranes containing designed nanochannel architectures obtained by pyrolysis of ion-track etched polyimide. Materials Chemistry and Physics, 2014, 148, 846-853.	4.0	11
279	Graphitization of amorphous carbon by swift heavy ion impacts: Molecular dynamics simulation. Diamond and Related Materials, 2018, 83, 134-140.	3.9	11
280	Borate-driven ionic rectifiers based on sugar-bearing single nanochannels. Nanoscale, 2021, 13, 11232-11241.	5.6	11
281	The colouration of CaF 2 crystals by keV AND GeV ions. Radiation Effects and Defects in Solids, 2002, 157, 637-641.	1.2	10
282	Cratering by MeV–GeV ions as a function of angle of incidence. Nuclear Instruments & Methods in Physics Research B, 2003, 206, 7-12.	1.4	10
283	Measurements of fossil confined fission tracks in ion-irradiated apatite samples with low track densities. Nuclear Instruments & Methods in Physics Research B, 2007, 259, 943-950.	1.4	10
284	Ion track lithography and graphitic nanowires in diamondlike carbon. Journal of Vacuum Science & Technology B, 2008, 26, 2468-2472.	1.3	10
285	Optimization of nanopores obtained by chemical etching on swift-ion irradiated lithium niobate. Nuclear Instruments & Methods in Physics Research B, 2009, 267, 1035-1038.	1.4	10
286	Two dimensional anisotropic etching in tracked glass. Journal of Materials Chemistry, 2009, 19, 8142.	6.7	10
287	Structure alterations in microporous (Mg,Fe)2Al4Si5O18 crystals induced by energetic heavy-ion irradiation. Journal of Solid State Chemistry, 2010, 183, 2372-2381.	2.9	10
288	Latent track radius of PTFE irradiated with high energy ion beam. Nuclear Instruments & Methods in Physics Research B, 2012, 273, 55-57.	1.4	10

#	Article	IF	CITATIONS
289	Annealing behaviour of ion tracks in olivine, apatite and britholite. Nuclear Instruments & Methods in Physics Research B, 2014, 326, 126-130.	1.4	10
290	Composition and orientation dependent annealing of ion tracks in apatite - Implications for fission track thermochronology. Chemical Geology, 2017, 451, 9-16.	3.3	10
291	Electronic sputtering of LiF, CaF 2 , LaF 3 and UF 4 with 197 MeV Au ions. Is the stoichiometry of atom emission preserved?. Nuclear Instruments & Methods in Physics Research B, 2017, 406, 501-506.	1.4	10
292	Radiation-induced disorder in compressed lanthanide zirconates. Physical Chemistry Chemical Physics, 2018, 20, 6187-6197.	2.8	10
293	Swift-heavy ion irradiation response and annealing behavior of A2TiO5 (A = Nd, Gd, and Yb). Journal of Solid State Chemistry, 2018, 258, 108-116.	2.9	10
294	TEM analysis of radiation effects in ODS steels induced by swift heavy ions. Nuclear Instruments & Methods in Physics Research B, 2021, 486, 1-10.	1.4	10
295	Scanning force microscopy of surface damage created by fast C60 cluster ions in CaF2 and LaF3 single crystals. Nuclear Instruments & Methods in Physics Research B, 2007, 256, 313-318.	1.4	9
296	Development of nanostructures for thermoelectric microgenerators using ion-track lithography. Electronics Letters, 2008, 44, 500.	1.0	9
297	ZrSi formation at ZrN/Si interface induced by ballistic and ionizing radiations. Nuclear Instruments & Methods in Physics Research B, 2012, 286, 266-270.	1.4	9
298	Sputtering yield of amorphous 13C thin films under swift heavy-ion irradiation. Nuclear Instruments & Methods in Physics Research B, 2013, 314, 34-38.	1.4	9
299	Thermal response of nanoscale cylindrical inclusions of amorphous silica embedded in α-quartz. Physical Review B, 2014, 90, .	3.2	9
300	Structural and compositional characterization of Bi1â^'Sb nanowire arrays grown by pulsed deposition to improve growth uniformity. Nuclear Instruments & Methods in Physics Research B, 2015, 365, 668-674.	1.4	9
301	Swift heavy ion-induced radiation damage in isotropic graphite studied by micro-indentation and in-situ electrical resistivity. Nuclear Instruments & Methods in Physics Research B, 2015, 365, 509-514.	1.4	9
302	Fluoropolymer-based nanostructured membranes created by swift-heavy-ion irradiation and their energy and environmental applications. Nuclear Instruments & Methods in Physics Research B, 2018, 435, 162-168.	1.4	9
303	Nanoscale Structuring in Confined Geometries using Atomic Layer Deposition: Conformal Coating and Nanocavity Formation. Zeitschrift Fur Physikalische Chemie, 2018, 232, 1147-1171.	2.8	9
304	Elucidating the roles of diffusion and osmotic flow in controlling the geometry of nanochannels in asymmetric track-etched membranes. Journal of Membrane Science, 2021, 618, 118657.	8.2	9
305	Conical Nanotubes Synthesized by Atomic Layer Deposition of Al2O3, TiO2, and SiO2 in Etched Ion-Track Nanochannels. Nanomaterials, 2021, 11, 1874.	4.1	9
306	ÂFabrication And Plasmonic Characterization Of Au Nanowires With Controlled Surface Morphology. Advanced Materials Letters, 2015, 6, 377-382.	0.6	9

#	Article	IF	CITATIONS
307	Electrochemical Deposition of PbSe1-xTex Nanorod Arrays Using Ion Track Etched Membranes as Template. Molecular Crystals and Liquid Crystals, 2004, 418, 21-27.	0.9	8
308	Damage creation in LiF and NaCl crystals irradiated with swift heavy ions at 8 and 300 K. Physica Status Solidi C: Current Topics in Solid State Physics, 2007, 4, 1105-1109.	0.8	8
309	Poly(vinylidene fluoride)-Based Ion Track Membranes with Different Pore Diameters and Shapes. SEM Observations and Conductometric Analysis. Electrochemistry, 2010, 78, 146-149.	1.4	8
310	Conductivity enhancement of ion tracks in tetrahedral amorphous carbon by doping with N, B, Cu and Fe. Nuclear Instruments & Methods in Physics Research B, 2012, 272, 280-283.	1.4	8
311	In-situ investigation of polyvinyl formal irradiated with GeV Au ions. Nuclear Instruments & Methods in Physics Research B, 2012, 272, 400-404.	1.4	8
312	Static elasticity of cordierite I: Effect of heavy ion irradiation on the compressibility of hydrous cordierite. Physics and Chemistry of Minerals, 2014, 41, 579-591.	0.8	8
313	Conducting ion tracks generated by charge-selected swift heavy ions. Nuclear Instruments & Methods in Physics Research B, 2016, 381, 76-83.	1.4	8
314	Surface Enhanced DNP Assisted Solid-State NMR of Functionalized SiO <sub>2</sub> Coated Polycarbonate Membranes. Zeitschrift Fur Physikalische Chemie, 2018, 232, 1173-1186.	2.8	8
315	Spatially resolved magnetic resonance studies of swift heavy ion induced defects and radiolysis products in LiF crystals. Nuclear Instruments & Methods in Physics Research B, 2019, 441, 70-78.	1.4	8
316	TEM analysis of ion tracks and hillocks produced by swift heavy ions of different velocities in Y3Fe5O12. Journal of Applied Physics, 2020, 127, .	2.5	8
317	Multi-scale investigation of heterogeneous swift heavy ion tracks in stannate pyrochlore. Journal of Materials Chemistry A, 2021, 9, 16982-16997.	10.3	8
318	Etched ion-track membranes as tailored separators in Li–S batteries. Nanotechnology, 2021, 32, 365401.	2.6	8
319	Strong atomic displacements around nitrogen in tantalum determined by energy-dispersive x-ray diffraction. European Physical Journal B, 1985, 62, 63-70.	1.5	7
320	Solvent induced track sensitization. Swelling and diffusion measurements. Nuclear Instruments & Methods in Physics Research B, 1994, 91, 157-161.	1.4	7
321	Effect of temperature on track formation by energetic heavy ions in lithium fluoride. Radiation Effects and Defects in Solids, 2001, 155, 127-131.	1.2	7
322	Flexible microchannels with integrated nanoporous membranes for filtration and separation of molecules and particles. , 0, , .		7
323	Combined high pressure and heavy-ion irradiation: a novel approach. Journal of Synchrotron Radiation, 2009, 16, 773-777.	2.4	7
324	Highly conductive ion tracks in tetrahedral amorphous carbon by irradiation with 30 MeV C60projectiles. New Journal of Physics, 2011, 13, 083023.	2.9	7

#	Article	IF	CITATIONS
325	Formation of the defect halo of swift heavy ion tracks in LiF due to spatial redistribution of valence holes. Physica Status Solidi (B): Basic Research, 2013, 250, 850-857.	1.5	7
326	On-line Raman spectroscopy of calcite and malachite during irradiation with swift heavy ions. Nuclear Instruments & Methods in Physics Research B, 2015, 365, 564-568.	1.4	7
327	Polymeric lithography editor: Editing lithographic errors with nanoporous polymeric probes. Science Advances, 2017, 3, e1602071.	10.3	7
328	Sculpting Nanoscale Functional Channels in Complex Oxides Using Energetic Ions and Electrons. ACS Applied Materials & Interfaces, 2018, 10, 16731-16738.	8.0	7
329	Magnetotransport measurements on Bi2Te3 nanowires electrodeposited in etched ion-track membranes. Journal of Physics and Chemistry of Solids, 2019, 128, 360-366.	4.0	7
330	Cu2O/TiO2 Nanowire Assemblies as Photocathodes for Solar Hydrogen Evolution: Influence of Diameter, Length and NumberDensity of Wires. Zeitschrift Fur Physikalische Chemie, 2020, 234, 1205-1221.	2.8	7
331	Direct formation of nitrogen-vacancy centers in nitrogen doped diamond along the trajectories of swift heavy ions. Applied Physics Letters, 2021, 118, .	3.3	7
332	Anisotropic diffusion in etched particle tracks studied by field gradient NMR. Magnetic Resonance Imaging, 1994, 12, 245-246.	1.8	6
333	Fast heavy ion induced VUV absorption in LiF crystals. Nuclear Instruments & Methods in Physics Research B, 2002, 191, 212-215.	1.4	6
334	Microfabrication of Chip-sized Scaffolds for Three-dimensional Cell cultivation. Journal of Visualized Experiments, 2008, , .	0.3	6
335	Conductometric Analysis for the Formation of Poly(Vinylidene Fluoride)-Based Ion Track Membranes. ECS Transactions, 2011, 35, 1-12.	0.5	6
336	In-situ electric resistance measurements and annealing effects of graphite exposed to swift heavy ions. Nuclear Instruments & Methods in Physics Research B, 2013, 314, 125-129.	1.4	6
337	Effect of electronic energy loss on ion track formation in amorphous Ge. Nuclear Instruments & Methods in Physics Research B, 2014, 326, 113-116.	1.4	6
338	Thermal defect annealing of swift heavy ion irradiated ThO2. Nuclear Instruments & Methods in Physics Research B, 2017, 405, 15-21.	1.4	6
339	Bond-Breaking Efficiency of High-Energy Ions in Ultrathin Polymer Films. Physical Review Letters, 2018, 121, 066101.	7.8	6
340	Single-ion induced surface modifications on hydrogen-covered Si(001) surfaces—significant difference between slow highly charged and swift heavy ions. New Journal of Physics, 2021, 23, 093037.	2.9	6
341	Analysis of nanometer-sized aligned conical pores using small-angle x-ray scattering. Physical Review Materials, 2020, 4, .	2.4	6
342	Search for superfluid Josephson effect. International Journal of Radiation Applications and Instrumentation Part D, Nuclear Tracks and Radiation Measurements, 1991, 19, 967-970.	0.5	5

#	Article	IF	CITATIONS
343	Solvent induced track sensitization. Role of amines. Nuclear Instruments & Methods in Physics Research B, 1996, 107, 393-396.	1.4	5
344	Influence of radiation damage on ruby as a pressure gauge. Physical Review B, 2010, 82, .	3.2	5
345	Morphology and annealing kinetics of ion tracks in minerals. EPJ Web of Conferences, 2012, 35, 03003.	0.3	5
346	Investigation of Nanopore Evolution in Track-Etched Poly(vinylidene fluoride) Membranes. Transactions of the Materials Research Society of Japan, 2012, 37, 223-226.	0.2	5
347	Ion-track membranes of fluoropolymers: Toward controlling the pore size and shape. Nuclear Instruments & Methods in Physics Research B, 2013, 314, 77-81.	1.4	5
348	Reply to "Comment on â€~Dense and nanometric electronic excitations induced by swift heavy ions in an ionic CaF2crystal: Evidence for two thresholds of damage creation' ― Physical Review B, 2013, 87, .	3.2	5
349	Orientation dependent annealing kinetics of ion tracks in c-SiO2. Journal of Applied Physics, 2015, 118, 224305.	2.5	5
350	Growth and morphological analysis of segmented AuAg alloy nanowires created by pulsed electrodeposition in ion-track etched membranes. Beilstein Journal of Nanotechnology, 2015, 6, 1272-1280.	2.8	5
351	Oxygen loss induced by swift heavy ions of low and high dE/dx in PMMA thin films. Nuclear Instruments & Methods in Physics Research B, 2015, 365, 578-582.	1.4	5
352	Ion track annealing in quartz investigated by small angle X-ray scattering. Nuclear Instruments & Methods in Physics Research B, 2015, 365, 380-383.	1.4	5
353	Study on structural recovery of graphite irradiated with swift heavy ions at high temperature. Nuclear Instruments & Methods in Physics Research B, 2015, 365, 522-524.	1.4	5
354	Low temperature annealing effects on the stability of Bi nanowires. Physica Status Solidi (A) Applications and Materials Science, 2016, 213, 603-609.	1.8	5
355	Nanometer collimation enhancement of ion beams using channeling effects in track-etched mica capillaries. Scientific Reports, 2017, 7, 17081.	3.3	5
356	Sputtering of LiF and other halide crystals in the electronic energy loss regime. European Physical Journal D, 2020, 74, 1.	1.3	5
357	Nanoparticle emission by electronic sputtering of CaF2 single crystals. Applied Surface Science, 2021, 537, 147821.	6.1	5
358	Ion irradiation induced strain and structural changes in LiTaO <sub>3</sub> perovskite*. Journal of Physics Condensed Matter, 2021, 33, 185402.	1.8	5
359	Ion track etching of polycarbonate membranes monitored by <i>in situ</i> small angle X-ray scattering. Physical Chemistry Chemical Physics, 2021, 23, 14231-14241.	2.8	5
360	Chemical conversions in lead thin films induced by heavy-ion beams at Coulomb barrier energies. Nuclear Instruments and Methods in Physics Research, Section A: Accelerators, Spectrometers, Detectors and Associated Equipment, 2022, 1028, 166365.	1.6	5

#	Article	IF	CITATIONS
361	XPS analysis of Cu/Teflon interface irradiated by heavy ions. Synthetic Metals, 1994, 67, 121-124.	3.9	4
362	Spatially resolved characterization of Xe ion irradiated LiF crystals using static field gradient NMR. Journal of Physics Condensed Matter, 2008, 20, 465215.	1.8	4
363	Track-etched nanopores in spin-coated polycarbonate films applied as sputtering mask. Nuclear Instruments & Methods in Physics Research B, 2009, 267, 1032-1034.	1.4	4
364	Luminescence of dye-doped KAP and KDP nanorods. Radiation Measurements, 2010, 45, 602-604.	1.4	4
365	Spatially resolved nuclear spin relaxation, electron spin relaxation and light absorption in swift heavy ion irradiated LiF crystals. Journal of Physics Condensed Matter, 2010, 22, 185402.	1.8	4
366	Transmission profiles of ions through nano-capillaries of rectangular cross-section in mica. Nuclear Instruments & Methods in Physics Research B, 2017, 406, 421-424.	1.4	4
367	Single Ion Track-Etched Nanochannels for Analytical Applications. , 2017, , 61-83.		4
368	Local structure and defects in ion irradiated KTaO <sub>3</sub> . Journal of Physics Condensed Matter, 2018, 30, 145401.	1.8	4
369	Selective transmembrane transport of $\hat{A^2}$ protein regulated by tryptophan enantiomers. Chemical Communications, 2021, 57, 215-218.	4.1	4
370	Force Microscopy of Heavy Ion Irradiated Materials. , 1995, , 489-494.		4
371	Desorption of polycyclic aromatic hydrocarbons by cosmic rays. Astronomy and Astrophysics, 2022, 663, A25.	5.1	4
372	Graphitic nanowires embedded in diamond-like carbon films. AIP Conference Proceedings, 2001, , .	0.4	3
373	Energy loss and fluence dependency of swift-ion-induced hardening in LiF. Physica Status Solidi C: Current Topics in Solid State Physics, 2005, 2, 434-437.	0.8	3
374	Tracks in epitaxial Si1â^'xGex alloy layers: Effect of layer thickness. Nuclear Instruments & Methods in Physics Research B, 2007, 256, 224-228.	1.4	3
375	Modifications of yttria fully stabilized zirconia thin films by ion irradiation in the inelastic collision regime. Journal of Applied Physics, 2008, 104, 093534.	2.5	3
376	Magnetic flux oscillations in partially irradiated Bi2Sr2CaCu2O8+δ crystals. Journal of Applied Physics, 2009, 105, 07E310.	2.5	3
377	Structural modifications induced by swift heavy ions in thin films of yttria fully stabilized zirconia. Nuclear Instruments & Methods in Physics Research B, 2010, 268, 3132-3136.	1.4	3
378	Conductive tracks of 30-MeV C60 clusters in doped and undoped tetrahedral amorphous carbon. Nuclear Instruments & Methods in Physics Research B, 2013, 307, 265-268.	1.4	3

#	Article	IF	CITATIONS
379	The influence of swift heavy ion irradiation on the recrystallization of amorphous Fe80B20. Microelectronic Engineering, 2013, 102, 64-66.	2.4	3
380	Static elasticity of cordierite II: effect of molecular CO2 channel constituents on the compressibility. Physics and Chemistry of Minerals, 2014, 41, 617-631.	0.8	3
381	Composition dependent thermal annealing behaviour of ion tracks in apatite. Nuclear Instruments & Methods in Physics Research B, 2016, 379, 211-214.	1.4	3
382	Selective Ionic Transport: Highly Selective Ionic Transport through Subnanometer Pores in Polymer Films (Adv. Funct. Mater. 32/2016). Advanced Functional Materials, 2016, 26, 5947-5947.	14.9	3
383	Modifications of gallium phosphide single crystals using slow highly charged ions and swift heavy ions. Nuclear Instruments & Methods in Physics Research B, 2016, 382, 86-90.	1.4	3
384	Conical etched ion tracks in SiO2 characterised by small angle X-ray scattering. Nuclear Instruments & Methods in Physics Research B, 2018, 435, 133-136.	1.4	3
385	Ion tracks in ultrathin polymer films: The role of the substrate. Current Applied Physics, 2021, 32, 91-97.	2.4	3
386	Heavy Ion Irradiation Effects on Structural and Ferroelectric Properties of HfO <sub>2</sub> Films. , 2020, , .		3
387	SWIFT HEAVY IONS IN MATTER. Nuclear Instruments & Methods in Physics Research B, 2009, 267, iii.	1.4	2
388	Guiding of slow Ne <sup>7+</sup> -ions through insulating nano-capillaries of various geometrical cross-sections. Journal of Physics: Conference Series, 2009, 194, 132030.	0.4	2
389	Synchrotron x-ray diffraction analysis of gadolinium and lanthanum titanate oxides irradiated by xenon and tantalum swift heavy ions. Materials Research Society Symposia Proceedings, 2015, 1743, 26.	0.1	2
390	Intense heavy ion beam-induced temperature effects in carbon-based stripper foils. Journal of Radioanalytical and Nuclear Chemistry, 2015, 305, 875-882.	1.5	2
391	Effect of ion velocity on creation of point defects halos of latent tracks in LiF. Nuclear Instruments & Methods in Physics Research B, 2017, 407, 80-85.	1.4	2
392	Annealing of ion tracks in apatite under pressure characterized in situ by small angle x-ray scattering. Scientific Reports, 2020, 10, 1367.	3.3	2
393	Desorption measurements of accelerator-related materials exposed to different stimuli. Vacuum, 2021, 194, 110608.	3.5	2
394	X-ray diffraction study of anharmonicity in Vsub3Si. Physical Review B, 1987, 35, 4193-4198.	3.2	1
395	<title>Heavy ion-induced damage and modifications of insulating materials</title> ., 2001, , .		1
396	Material modifications induced by swift heavy ions in NbTi superconducting wires. Phase Transitions, 2008, 81, 285-292.	1.3	1

#	Article	IF	CITATIONS
397	Efficient field emission of gold and platinum nanowire patch arrays. , 2009, , .		1
398	Structural changes in thin films of yttria-stabilized zirconia irradiated with uranium ions in the electronic stopping regime. Journal of Nuclear Materials, 2011, 416, 173-178.	2.7	1
399	Optimization of ion-track etching and electrochemical Cu nanocone deposition for field emission cathodes. , 2012, , .		1
400	Projected length annealing of etched 152Sm ion tracks in apatite. Nuclear Instruments & Methods in Physics Research B, 2012, 288, 48-52.	1.4	1
401	Swift Heavy Ion-Induced Decomposition and Phase Transformation in Nanocrystalline SnO2. Materials Research Society Symposia Proceedings, 2014, 1715, 13.	0.1	1
402	Transmission of highly charged ions through nanocapillaries of noncircular cross sections. Journal of Physics: Conference Series, 2014, 488, 012035.	0.4	1
403	Electrical conduction of ion tracks in tetrahedral amorphous carbon: temperature, field and doping dependence and comparison with matrix data. New Journal of Physics, 2015, 17, 123009.	2.9	1
404	In situ Resonant Ultrasound Spectroscopy during irradiation of solids with relativistic heavy ions. Acta Materialia, 2015, 89, 60-72.	7.9	1
405	Characterization of Radiation Effects and Ion Tracks with Spallation Neutron Probes. Nuclear Physics News, 2020, 30, 16-19.	0.4	1
406	Dynamic Response of Graphitic Targets with Tantalum Cores Impacted by Pulsed 440-GeV Proton Beams. Shock and Vibration, 2021, 2021, 1-19.	0.6	1
407	Chemical degradation of polyimide and polysulfone films under the irradiation with heavy ions of several hundred meV. , 1999, 37, 4318.		1
408	Energy Deposition by Ultrahigh Energy Ions in Large and Small Sensitive Volumes. IEEE Transactions on Nuclear Science, 2022, 69, 241-247.	2.0	1
409	UV-induced Caribbean transition in punch-treated organic structures. Nuclear Instruments & Methods in Physics Research B, 1995, 105, x.	1.4	0
410	<title>Formation of dislocations and hardening of LiF crystals irradiated with energetic Au, Bi, Pb,&lt;br&gt;and S ions</title> . , 2003, 5122, 15.		0
411	FAIR Experiments in Biophysics and Materials Research. Nuclear Physics News, 2006, 16, 36-37.	0.4	Ο
412	Field emission properties of gold nanowire cathodes based on polymer ion-track membranes. , 2007, , .		0
413	Nimb Editorial for 2007. Nuclear Instruments & Methods in Physics Research B, 2007, 254, 1-2.	1.4	0
414	NIMB Editorial for 2008. Nuclear Instruments & Methods in Physics Research B, 2008, 266, 1.	1.4	0

#	ARTICLE	IF	CITATIONS
415	P2–21: Correlation between field emission current limits and morphology changes of gold nanowire patches. , 2010, , .		0
416	Self-aligned nanowires in tetrahedral amorphous carbon multilayer structures. , 2011, , .		0
417	Direct manipulation of the uncompensated antiferromagnetic spins in exchange coupled system by GeV ion irradiation. Applied Physics Letters, 2012, 100, 253102.	3.3	0
418	Modification of Fe-B based metallic glasses using swift heavy ions. EPJ Web of Conferences, 2012, 35, 03004.	0.3	0
419	Sharp bare and gold-coated copper nanocones with improved field emission performance. , 2013, , .		0
420	Transmission of slow highly charged ions through rectangular nanocapillaries. Journal of Physics: Conference Series, 2014, 488, 132043.	0.4	0
421	Density effects on the blocking of ions guided through insulating PET capillaries. Journal of Physics: Conference Series, 2014, 488, 132010.	0.4	0
422	Material-related issues at high-power and high-energy ion beam facilities. Journal of Physics: Conference Series, 2015, 599, 012039.	0.4	0
423	Swift Heavy Ions in Matter. Nuclear Instruments & Methods in Physics Research B, 2015, 365, 435-436.	1.4	0
424	Phase transformation and chemical decomposition of nanocrystalline SnO2 under heavy ion irradiation. Nuclear Instruments & Methods in Physics Research B, 2017, 407, 10-19.	1.4	0
425	Surface and subsurface damage in 14 MeV Au ion-irradiated diamond. Journal of Applied Physics, 2021, 130, 105303.	2.5	0
426	Dynamic Radiation Effects Induced by Short-Pulsed GeV U-Ion Beams in Graphite and h-BN Targets. Shock and Vibration, 2021, 2021, 1-11.	0.6	0
427	The iNAPO Project: Biomimetic Nanopores for a New Generation of Lab-on-Chip Micro Sensors. , 0, , .		0